Title
A PRIMER ON RECONSTRUCTION ALGORITHMS

Author
Budinger, T.F.

Publication Date
1978-09-01

Lawrence Berkeley Laboratory
UNIVERSITY OF CALIFORNIA

Presented at the World Federation of Nuclear Medicine and Biology, Washington, D.C., September 17-21, 1978

A PRIMER ON RECONSTRUCTION ALGORITHMS

T.F. Budinger

September 1978

Biology & Medicine Division

Prepared for the U.S. Department of Energy under Contract W-7405-ENG-48

A PRIMER ON RECONSTRUCTION ALGORITHMS

T. F. Budinger

Donner Laboratory
Lawrence Berkeley Laboratory
University of California
Berkeley, CA 94720

September 1978

This work was supported by the U.S. Department of Energy under Contract No. W-7405-ENG-48.

Lawrence Berkeley Laboratory
Report LBL-8212
September 1978

A PRIMER ON RECONSTRUCTION ALGORITHMS

T. F. Budinger
Donner Laboratory
University of California

Table of Contents

Prepared for World Fed.
of Nuclear Medicine
and Biology, Sept. 1978

A PRIMER ON RECONSTRUCTION ALGORITHMS

T. F. Budinger
Donner Laboratory
University of California

INTRODUCTION AND PURPOSE

The subject of reconstruction algorithms includes the arithmetic or computational methods whereby projection data are manipulated to form transverse section images. Algorithms for reconstruction tomography include not only methods for transverse section reconstruction but also methods for longitudinal tomography; that is, the computational methods of presenting images from data obtained by the Anger tomoscanner as well as the methods for multiple pin hole tomography and Fresnel zone plate tomography. At the outset this whole field of reconstruction tomography seems so complex that a general understanding of the methods is frequently left to the computer or mathematically oriented researchers in nuclear medicine. It is the intent of this portion of the course to show how simple reconstructive tomography is accomplished and at the same time to present some insight into the general problem so that the participant can better judge and contribute to the ongoing research in this field. This booklet consists of a few exercises which the participant will be asked to go through as part of the presentation. At the conclusion of the presentation this booklet should contain sufficient information for review and subsequent teaching by the participant on reconstruction tomography.

DEFINITIONS

Definitions of various terms important for reconstructive tomography are given in general terms below in an order designed to help the participant gain some intuition about reconstruction principles.

1. PROJECTION: The result of summing the activity along lines through the object. The usual Anger camera image is a two-dimensional projection of activity through the body. One-dimensional projections are formed by summing the activity or density along parallel lines through a plane or a transverse section.

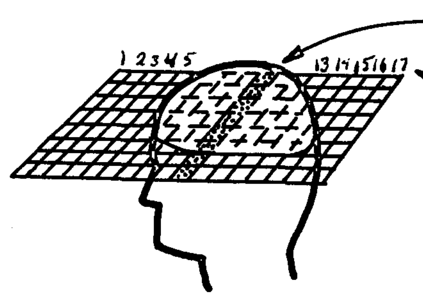

Summation of activity along this line or ray gives the one value of the one dimensional projection. Each value is put in a projection bin number for each angle.

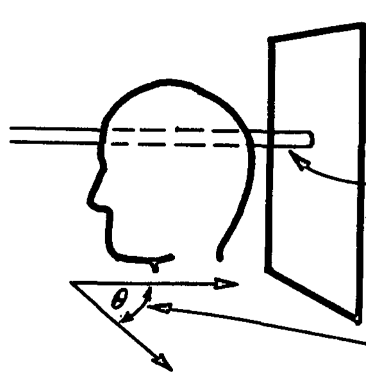

Summation of activities along this path gives one value of the 2D projection for the three dimensional object

Projection angle

2. MULTIPLE ANGLES OR MULTIPLE VIEWS:

In the context of ECT this term implies multiple projections from different viewpoints around an object.

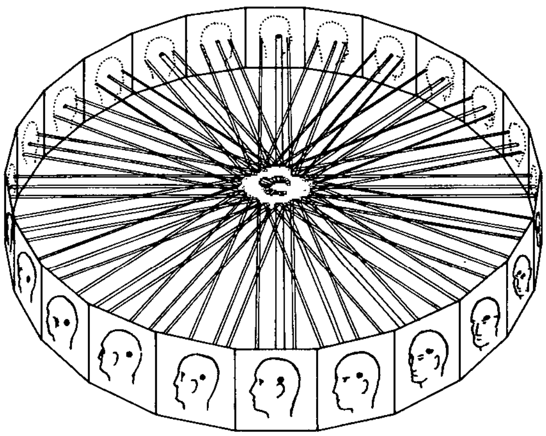

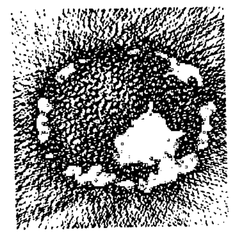

Data from multiple angles can be obtained by rotation of a patient in front of a detector such as an Anger camera, or by rotation of the camera around the patient, or by surrounding the patient by detectors

SINGLE PHOTON DEVICES

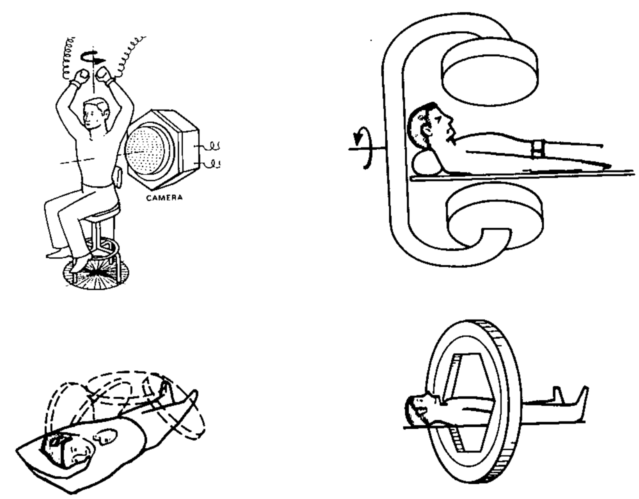

FOUR ANGER CAMERA VIEWS

ARC OR HEXAGONAL COLLIMATED CRYSTAL ANNULUS

or by moving a pinhole to several positions or by manipulating data from coded apertures.

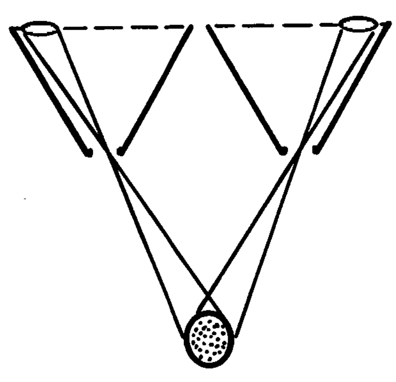

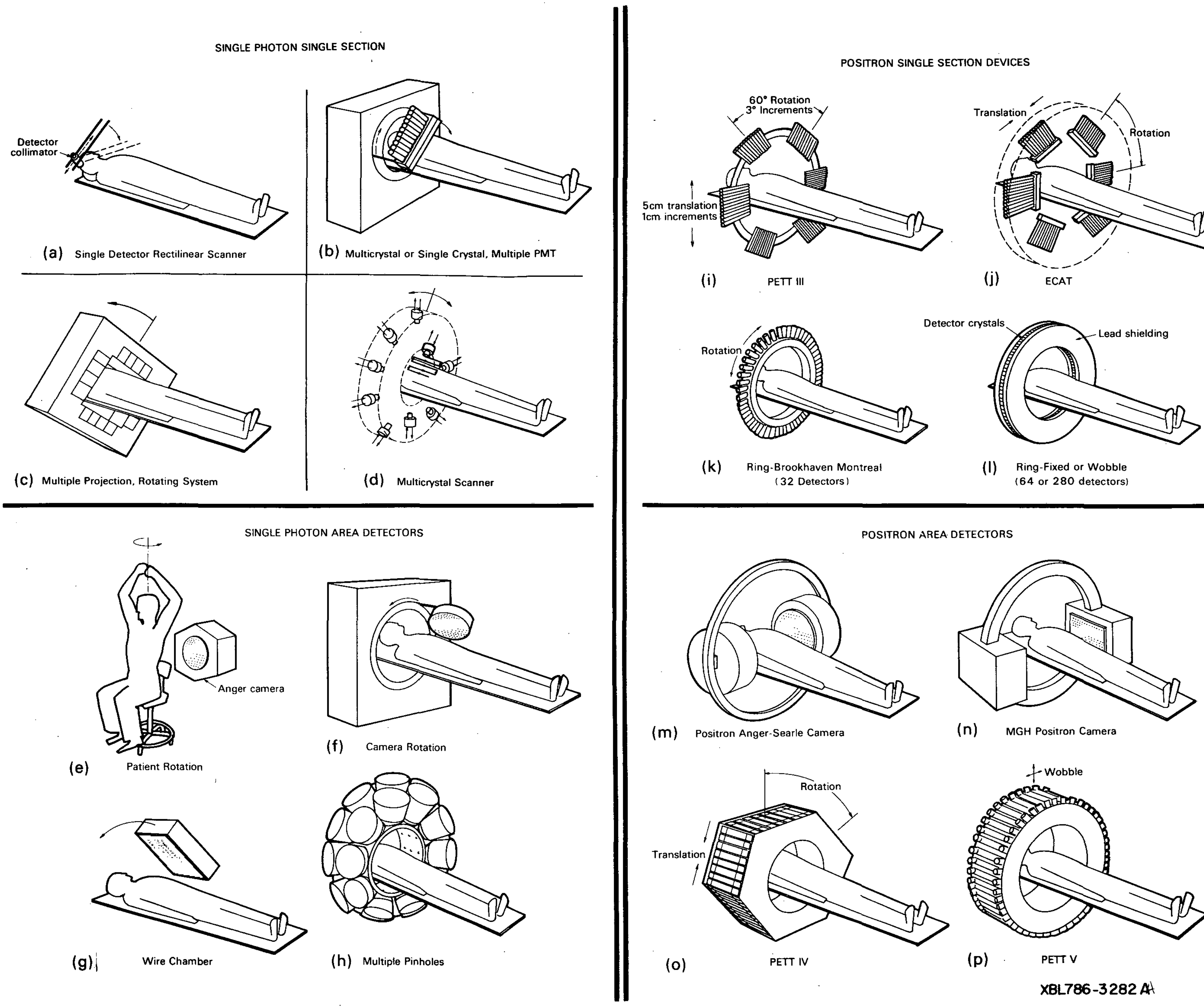
SINGLE PHOTON SINGLE SECTION
Detector collimator
(a) Single Detector Rectilinear Scanner
(b) Multicrystal or Single Crystal, Multiple PMT
(c) Multiple Projection, Rotating System
(d) Multicrystal Scanner
SINGLE PHOTON AREA DETECTORS
Anger camera
(e) Patient Rotation
(f) Camera Rotation
(g) Wire Chamber
(h) Multiple Pinholes
POSITRON SINGLE SECTION DEVICES
60° Rotation
3° Increments
5cm translation
1cm increments
(i) PETT III
Translation
Rotation
(j) ECAT
Rotation
(k) Ring-Brookhaven Montreal
(32 Detectors)
Detector crystals
Lead shielding
(l) Ring-Fixed or Wobble
(64 or 280 detectors)
POSITRON AREA DETECTORS
(m) Positron Anger-Searle Camera
(n) MGH Positron Camera
Rotation
Translation
(o) PETT IV
Wobble
(p) PETT V
XBL786-3282 A

3. BACK-PROJECTION:

The process whereby projection data are put back through the image space for each angle. As data from one angle overlap data from another angle in various picture elements the data are merely summed. The result is a blurred image. Refer to the top figure of page 2 and imagine projecting the views from multiple angles back through the space where the object originated. The result is a blurred image of the original object. An example of the operation for only 3 views is shown below.

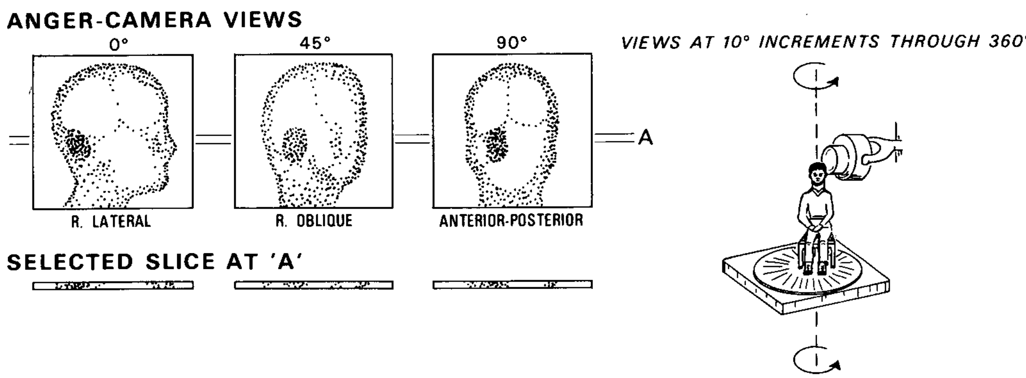

Profiles or projection arrays at a selected level are "back projected" through an empty array but rotated in accord with the projection angle. Below are three separate arrays resulting from this process.

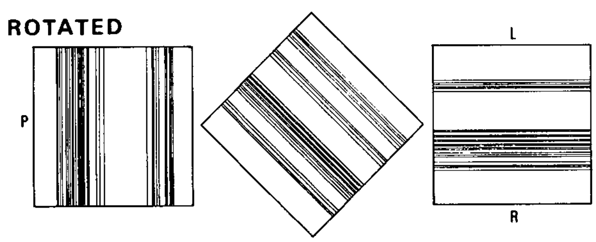

Then the three arrays are simply added together which is the same as superposition.

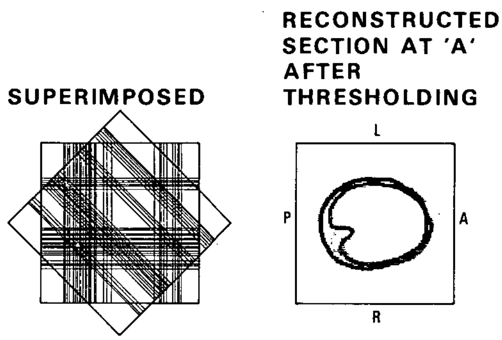

The same result can be obtained by back projecting the projection profiles through a single image array and adding the data from each projection bin to each image picture element the projection bin value or ray passes through. Note that this process results in a blurring of the original image as can be seen for an infinite number of views below.

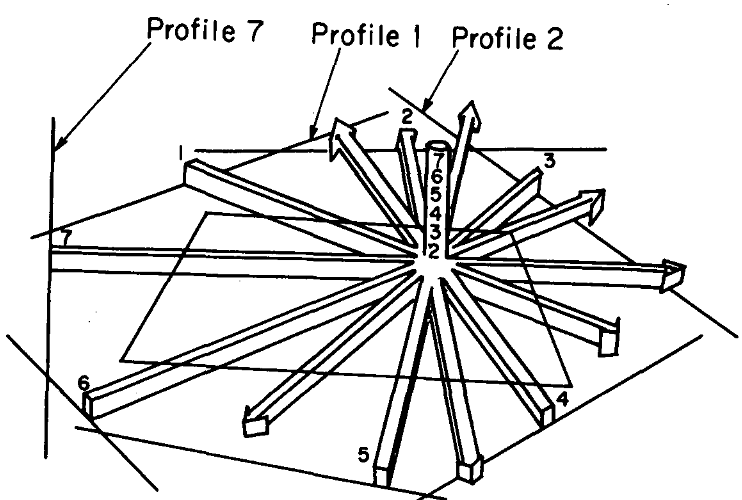

Back projection of seven profiles

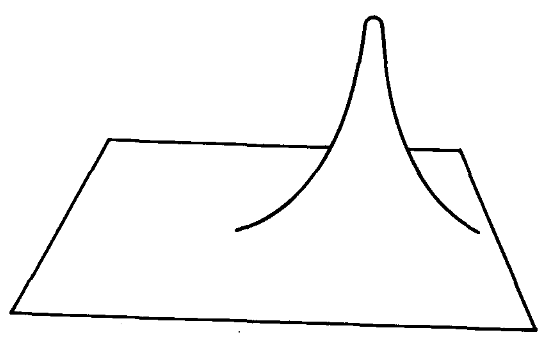

Back projection of an infinite number of projections

4. SIMPLE SUPERPOSITION: A process whereby the back-projection is formed.

5. DE-BLURRING: The process whereby the blurred image is filtered using a convolution or Fourier Transform filter algorithm.

6. REAL SPACE: The 3-D space we know naturally when described by the mathematician is called real space, configuration space or cartesian space, and describes the object density or activity in terms of x,y,z coordinates or in terms of a radius (r), elevation or height (ϕ), and azimuthial angle (θ).

7. FOURIER SPACE:

The space wherein the frequency rather than the distance is used as the coordinates. Consider a two dimensional image of a bar pattern with bars separated from center to center by 2 centimeters. The Fourier space representation of this pattern would also be a two dimensional pattern but the 2-cm wavelength of the bars would be represented as an amplitude at a frequency of 1 wavelength/2 cm = 0.5 cm^{-1}.

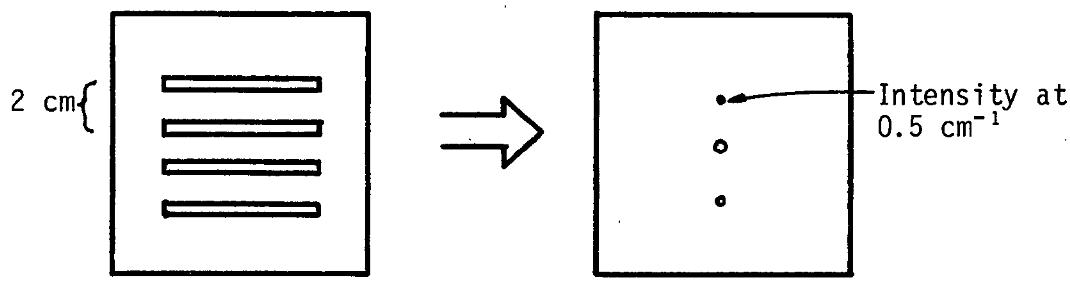

Now consider a pattern with bars closer together, e.g., at 1 cm as well as bars at a wavelength of 2 cm but in another direction.

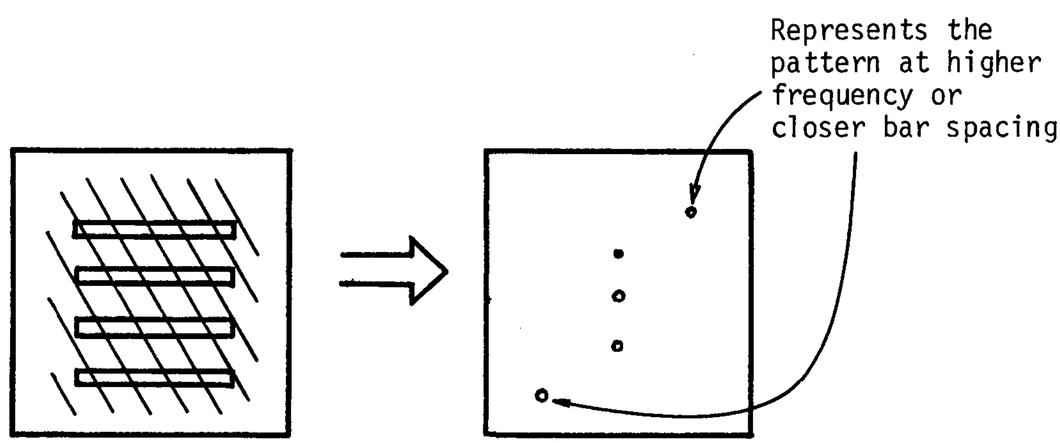

See also the definition of Fourier transform.

8. FOURIER TRANSFORMATION:

The mathematical process whereby the real space representation of an object in one, two or three dimensions is transformed into the Fourier space representation. The transformation is done by mathematically breaking up the object into a series of sinusoidal waveforms of different frequencies. The summation of these sinusoidal waves gives back the original object.

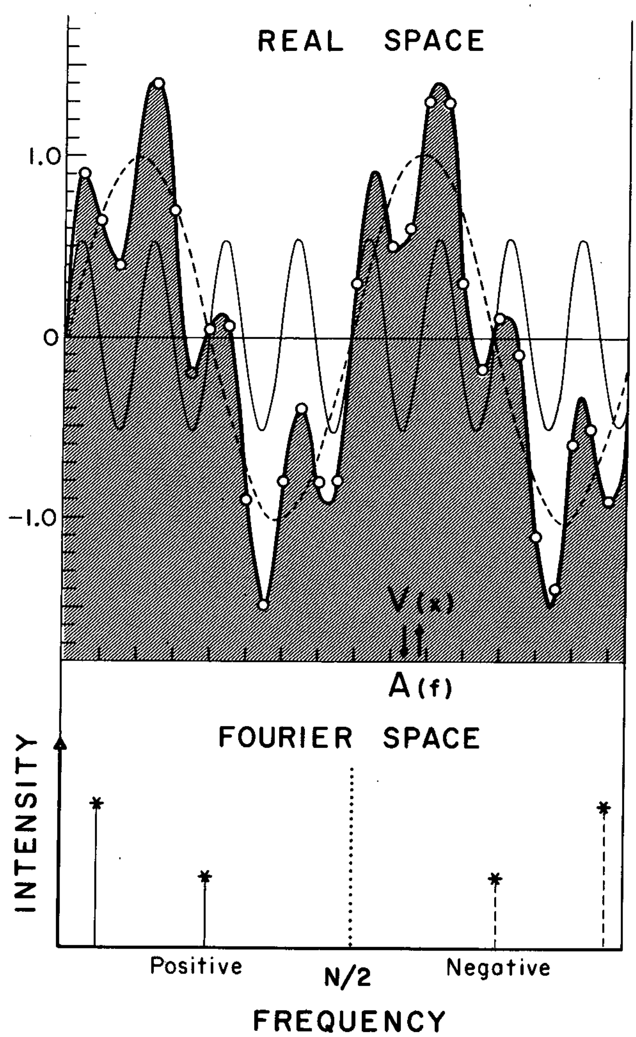

XBL694-2573

9. CONVOLUTION:

The result of convolving or folding one function with another whereby the peaks and valleys of a function or profile can be sharpened or smoothed depending on which convolving function is used. The mathematical operation for discrete data such as we have in computed tomography is symbolized as

$$P_{new}(K) = \sum_{n=1}^{\infty} h(K - n)\, P_{old}(n)$$

Here h is the kernel (filter)
where P_{old} is the original data for the various bins denoted by n and P_{new} is the new or convolved profile array at bin values denoted by K.

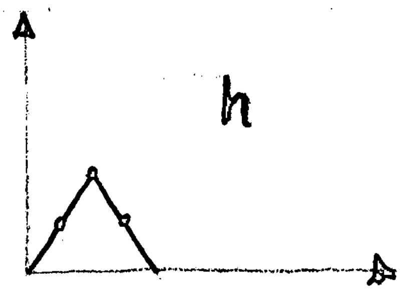

Suppose $h(1) = +\frac{1}{4}$

$h(2) = +\frac{1}{2}$

$h(3) = +\frac{1}{4}$

and we have a projection array with values

P(1) = 0

P(2) = 1

P(3) = 1

P(4) = 1

P(5) = 1

P(6) = 0

P(7) = 0

P(8) = 0

.
.
.
.
.

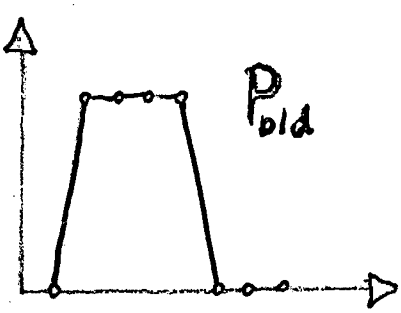

The convolution operation follows the equation as shown by a few examples below.

$$P(2) = \sum_{n=1}^{\infty} h(2-n)\, P(n)$$

$$= h(1)\,P(1) + h(0)\,P(2) + h(-1)\,P(3) + h(-2)\,P(4) + h(-3)\,P(5)$$

$$+\ h(-4)\,P(6) + h(-5)\,P(7) + h(-6)\,P(8) = 0$$

$$P(4) = \sum_{n=1}^{\infty} h(4-n)\, P(n)$$

$$= h(3)\,P(1) + h(2)\,P(2) + h(1)\,P(3) + h(0)\,P(4) + h(-1)\,P(5)$$

$$+\ h(-2)\,P(6) + h(-3)\,P(7) + h(-4)\,P(8) = 0 + \tfrac{1}{2} + \tfrac{1}{4} + 0 = 3/4$$

The result is:

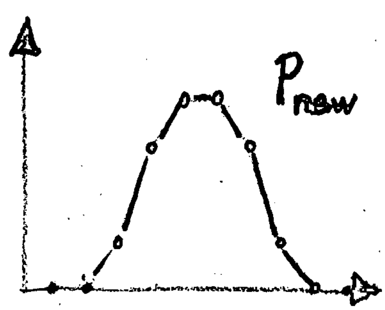

$P(1) = 0$

$P(2) = 0$

$P(3) = \frac{1}{4}$

$P(4) = 3/4$

$P(5) = 1$

$P(6) = 1$

$P(7) = 3/4$

$P(8) = \frac{1}{4}$

10. KERNEL:

The particular function used as the convolving function. For example, a smoothing kernel might have values of ¼, ½, ¼. (These are frequently known as weighting values.) In the case of a projection profile which we might want to smooth to get rid of noise this smoothing kernel would be used in a convolution calculation. In the case of reconstruction tomography the kernel is a sharpening kernel such as -¼, 1, -¼. Note that the convolution operation with this kernel on a projection array will result in each bin value being modified by subtracting from it ¼th the values of the bin value on either side. For two dimensions the kernel is two-dimensional; for example, 3 x 3 picture smoothing can be accomplished by a kernel with weightings of ¼ in the center and 1/16 the surrounding eight elements.

11. CONVOLUTION THEOREM:

A mathematical theorem which proves the equivalence between convolutions in real space and taking products of the Fourier transform of the kernel and the Fourier transform of the function being convolved. If h is the kernel or the smoothing function, and P is the profile function then the convolution of h with P is symbolized as

$$P_{new}(x) = \int h(x - x')\, P_{old}(x')\, dx'$$

or for the discrete cases we deal with in practice

$$P_{new}(k) = \sum_{n=o}^{\alpha} h(k - n)\, P_{old}(n).$$

The convolution theorem says that the Fourier transform of P_{new} is equal to the product of the Fourier transform of the kernel and the Fourier transform of P_{old}; thus

$$\mathscr{F}(P_{new}) = \mathscr{F}(h) \times \mathscr{F}(P_{old})$$

Since P_{new} is the inverse Fourier transform of (P_{new}) we have a method of performing the convolution operation by simply multiplying Fourier transforms of h and p and taking the inverse transform of the result.

12. FFT or FAST FOURIER TRANSFORMATION:

A method of rapidly computing the Fourier transform of a function. For profiles which are 64 points long and kernels about 32 points long it is faster to do a convolution by the convolution theorem method rather than the direct multiplication and additions required by the convolution recipe given in definition 9 above.

13. FILTERING:

Sometimes used synonymously with convolution but more precisely defined as a method by which the sine and cosine terms of the Fourier transform of the function are either amplified or depressed in order to get the same result as one would get by doing a convolution.

14. FILTER:

The particular modifying function used in the filtering operation.

15. RAM-LAK FILTER:

Ramachandran and Lakshminarayanan proposed a convolution kernel in 1971 which allowed one to de-blur the blurring of back projection.

16. SHEPP-LOGAN FILTER:

Shepp and Logan proposed a convolution filter which included a smoothing kernel in the convolution kernel of the RAM-LAK Filter. Chesler from MGH proposed a similar filter for nuclear medicine.

17. RAMP FILTER:

The shape of the Fourier transform of the RAM-LAK filter is a ramp in frequency space. That is, the value of the filter increases in direct proportion to the frequency.

18. ATTENUATION:

The modulation of the intensity of an isotopic source due to Compton scattering and photoelectric absorption. The attenuation of photons from a source of positrons 10 cm deep in the body is calculated by

$$I(d = 10) = I_o e^{-\mu 10} = \frac{I}{I_o} = e^{-0.098 \cdot 10} = 0.375$$

That is, only 37.5% will leave the object.

19. SINGLE PHOTON EMISSION COMPUTED TOMOGRAPHY:

Computed tomography using non-positron emitting sources such as ^{123}I and ^{99}Tc labeled radiopharmaceuticals.

20. POSITRON EMISSION COMPUTED TOMOGRAPHY:

Computed tomography using radionuclides which decay by positron ejection, from ^{11}C, ^{13}N, ^{15}O, ^{18}F, ^{52}Fe, ^{68}Ga, ^{77}Kr, ^{82}Rb, etc. The positron travels a very short range in tissue then, upon encountering an electron, the two particles annihilate and two photons of 511 keV energy are released in opposite directions. Page 3 shows various configurations and the diagram below illustrates the concept. PETT stands for positron emission transaxial tomograph.

21. EMISSION COMPUTED TOMOGRAPHY:

The method of calculating transverse sections from multiple views of some portion of the body.

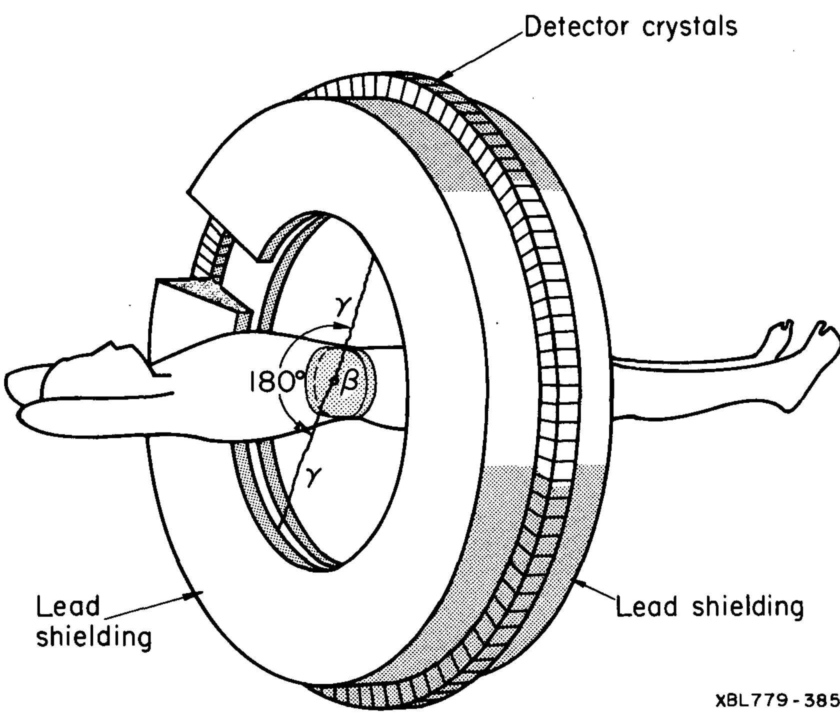

XBL779-3850

ESSENCE OF RECONSTRUCTION METHODS

The main task, indeed the essence of computed tomography, is to remove or filter the blurring from the back projection image. Recall that simple back projection of projection profiles gives only a blurred or smeared representation of the true object because, as shown on Page 4, each point in the reconstructed transverse section will consist of the superposition of a set of straight lines corresponding to each projection value from that point in the true object. The resulting back projection image is a convolution (see Def. 2) of the true distribution with a kernel which smooths each point by a weighting value which is inversely proportional to the distance from that point. This results in an image which appears like the true transverse section but with thick syrup poured over it. Mathematically we represent this as

$$B(x,y) = \iint \frac{A(x',y')}{\{(x-x')^2 + (y-y')^2\}^{\frac{1}{2}}} dx'dy' = A * r^{-1}$$

where B is a back projected image and A is the true image. Here * signifies a convolution. This smearing results in the middle image of the figure below, which is a simulation of the heart and lungs in the thorax.

Since we know the image smoothing kernel (i.e., the character of the syrup) we can find the kernel to unsmooth the back projection image (i.e., the solution to dissolve the syrup). This de-blurring function is applied to the blurred image to give the result shown in panel three below.

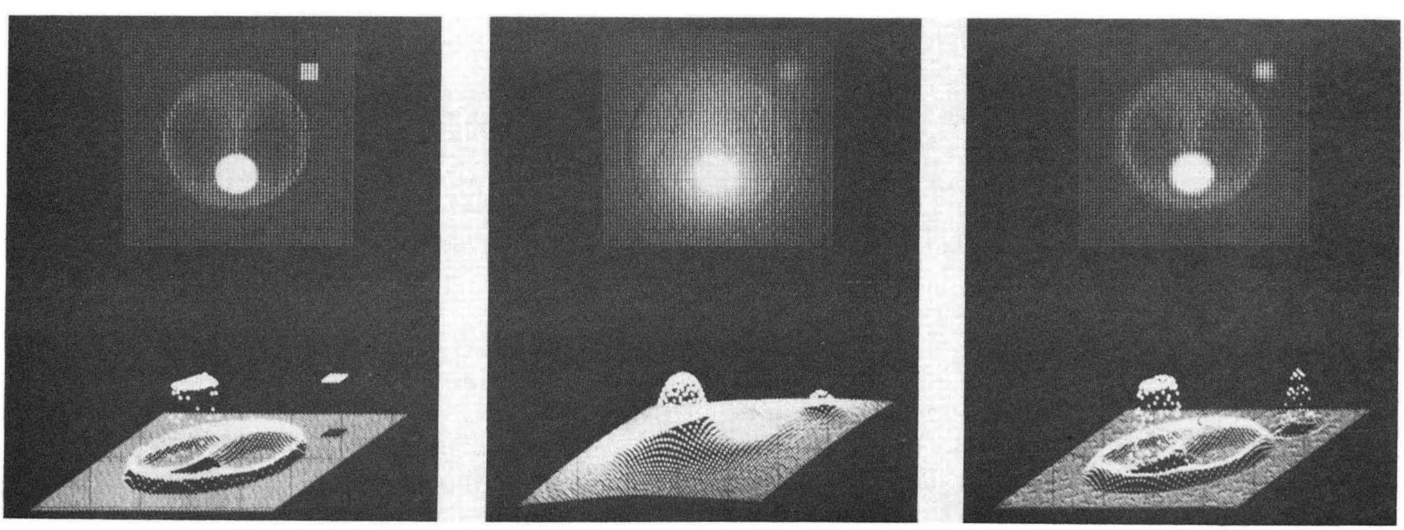

Original Superposition Filtered

DE-BLURRING THE PROJECTIONS OR THE BACK PROJECTION IMAGE

Thus far we have looked at the problem of de-blurring from the viewpoint of de-convolving the blurring from the back projection image. However, it has been proved by Budinger and Gullberg (1975) that it makes no difference whether you de-blur the back projection image or de-blur the projections before performing the back projection. As it turns out, it is easier to de-blur the projections, then perform the back projection. A method of de-blurring the projections is to convolve the values along each projection with a sharpening "filter" or kernel of the Shepp-Logan or Chesler type. We obtain the same result if we use one of these filters on the back projection image.

SIX BASIC CLASSES OF

RECONSTRUCTION ALGORITHMS

Categories into which the reconstruction methods can be organized are listed in order of popularity.

1. CONVOLUTION TECHNIQUE
2. FILTERED BACK PROJECTION
3. ITERATIVE METHODS
4. FOURIER PROJECTION THEOREM METHOD
5. DIRECT OR GENERALIZED INVERSE
6. OPTICAL METHODS

In this section we will discuss each method and perform small exercises on the first 3 techniques in order to achieve a better insight into their operations.

1. CONVOLUTION TECHNIQUE:

The projection data are convolved with a kernel which acts like taking the first derivative of the projection function. The kernel can be of the RAM-LAK or SHEPP-LOGAN type.

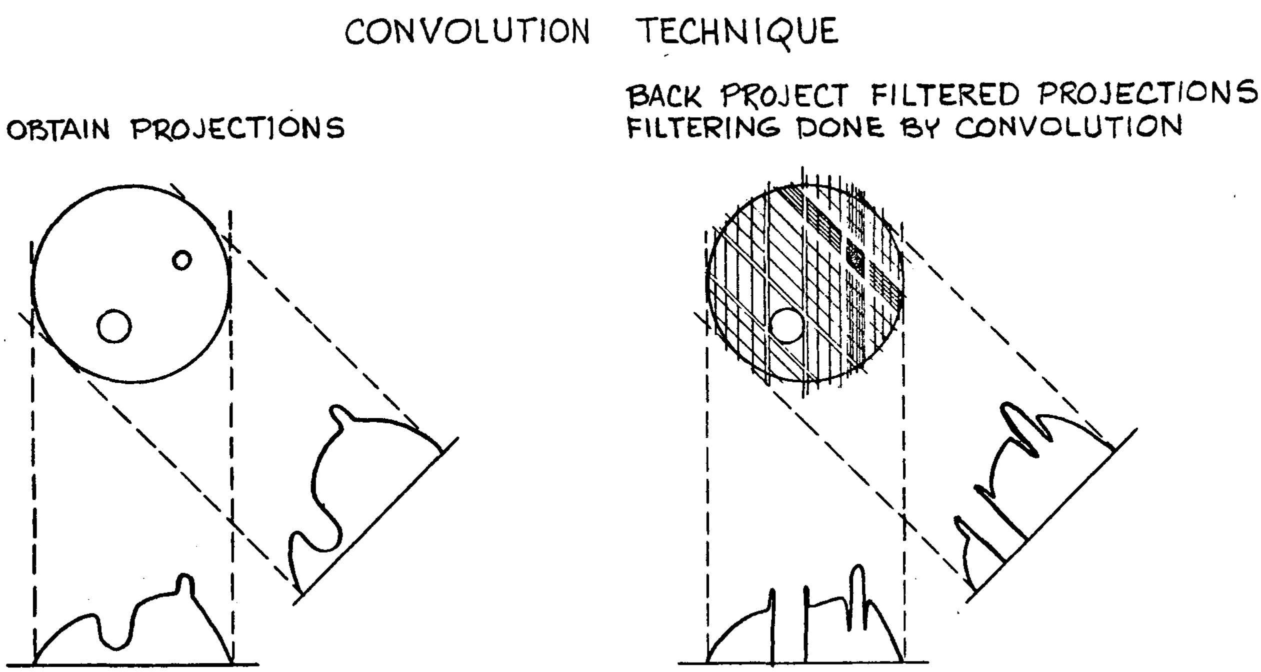

Exercise I - Given the following projections

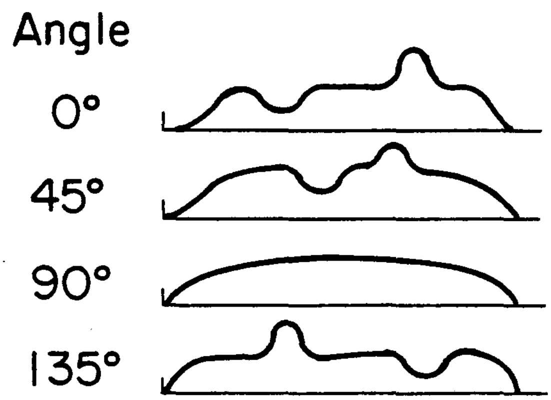

Profiles

Reconstruct the original object

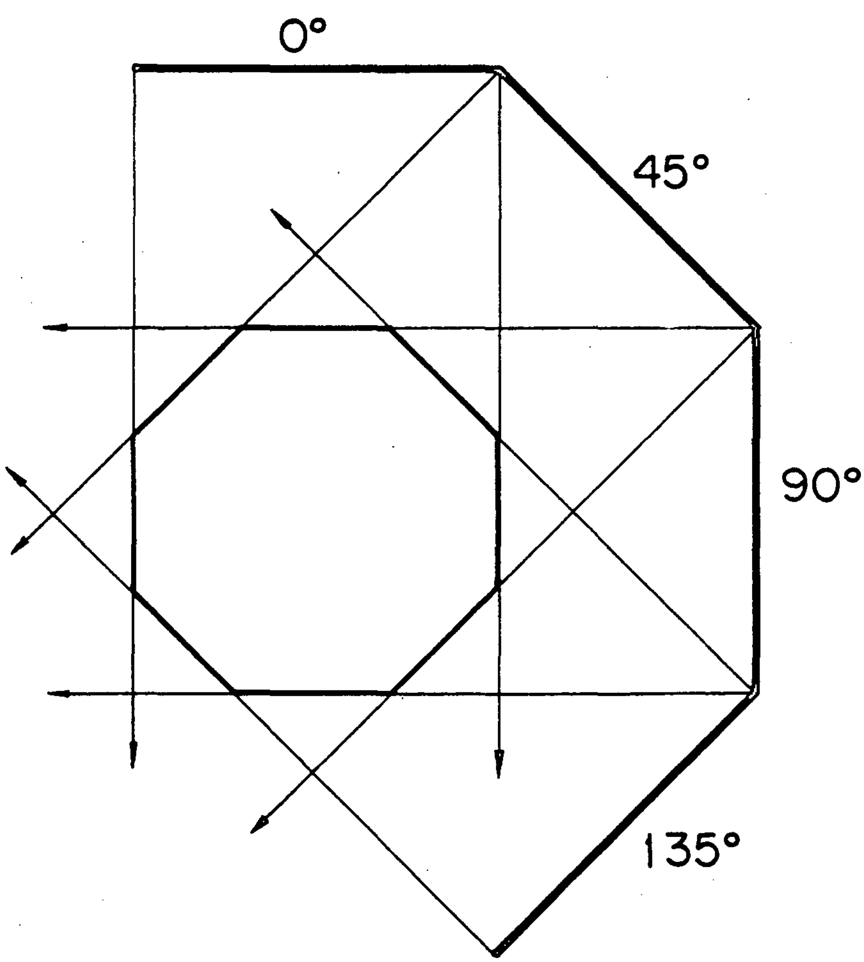

XBL789-3525

2. FILTERED BACK PROJECTION:

The projection data and the kernel are Fourier transformed. The product of these 2 Fourier transforms is formed and the result is inversely transformed. This is equivalent to the convolution technique. At Donner Laboratory we use this technique because it allows us to change the filter shape such that we can control the frequencies which are being modified.

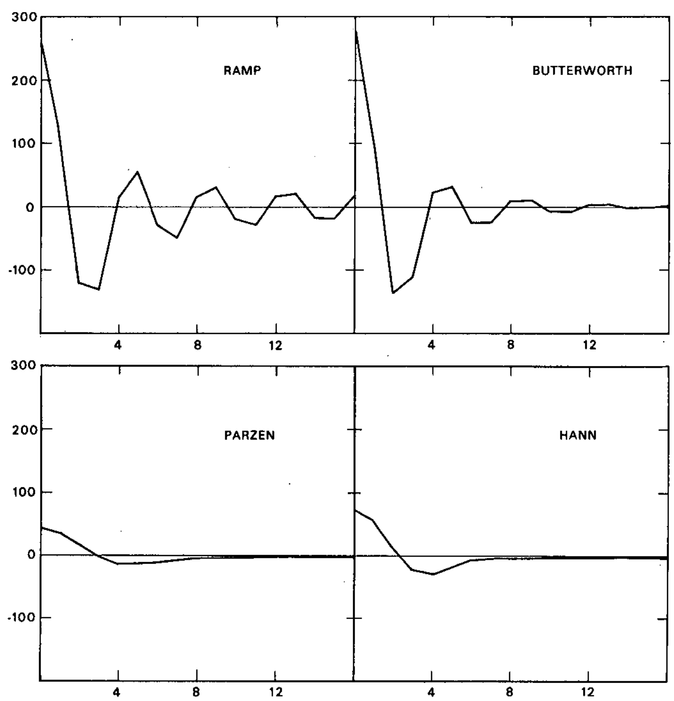

SHAPE OF THE REAL
SPACE KERNELS

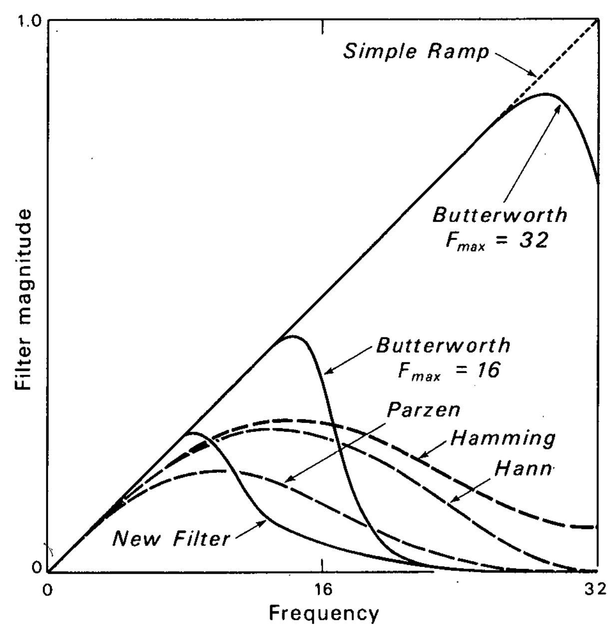

SHAPE OF THE
FREQUENCY SPACE FILTERS

EXERCISE II

Given the following definitions:

$P_{k\theta}$	Projection profile
k	Bin number along the profile
θ	Angle
h	Kernel
BP	Back projection operation
$\mathscr{F}_1$	Fourier transformation in one dimension
$\mathscr{F}_2$	Fourier transformation in two dimensions
Σ	Summation
x	Multiplication
*	Convolution
$\lvert R \rvert$	Ramp filter

Show by symbols how the Filtered back projection technique is executed for a ramp filter.

Example: The way to symbolize the convolution technique is:

$$h * P_{k\theta} \quad \text{for each } \theta$$

$$BP\ (h * P_{k\theta}) \text{ for each } \theta$$

$$\sum_{\theta} \{BP\ (h * P_{k\theta})\} \text{ for all } \theta\text{'s.}$$

Show the method by putting down the first operation on the right and then move left as was done in the example.

3. ITERATIVE METHODS:

The arithmetic techniques known as ART (algebraic reconstruction technique); SIRT (simultaneous iterative reconstruction technique); OTC (orthogonal tangent correction technique); and ILST (iterative least squares technique) all belong to the class of algorithms which creep up on an answer by successive smart guesses at the value for the image picture element. The basic idea is to assume on the first iteration that the true image is the back projection image. Next we reproject the back projection image and compare the results of the reprojection of each projection ray to the actual measured data. At the first iteration there will be a discrepancy between the calculated projection and the true data; that is

$$\text{Calculated} - \text{True} \neq 0 \qquad \text{for each bin of each angle}$$

or

$$\frac{\text{Calculated}}{\text{True}} \neq 1 .$$

To change the guess of the first iteration we multiply each picture element along the particular ray being examined by a factor to put the ray sum or reprojection value equal that of the true data value. Suppose

$$\frac{\text{Calculated}}{\text{True}} = 5/3$$

then we change each pixel along the ray corresponding to the value of 5 by 3/5

$$\text{Factor} = \frac{\text{True}}{\text{Calculated}} = 3/5$$

$$\text{Factor} \times \frac{\text{Calculated}}{\text{True}} = 1 .$$

In the exercise on Page 21 we are going to calculate the most likely activity distribution in a transverse section of a head wherein we have only 2 projections with only 2 bins per projection.

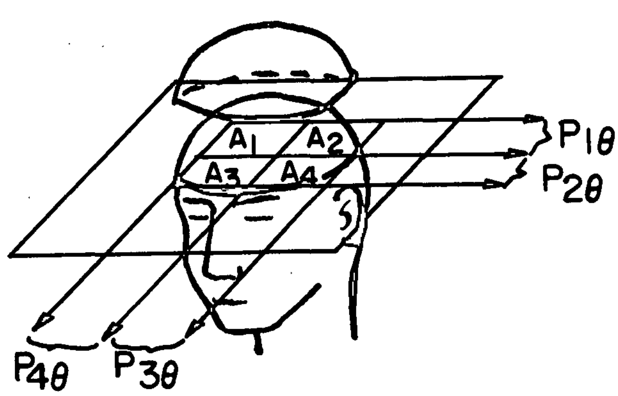

The technique we are to perform in the exercise on the next page is known as multiplicative ART and was one of the first techniques used on the EMI machine.

Iterative methods are not used in x-ray CT but are useful for emission CT in order to incorporate weighting based on noise or the attenuation coefficients for attenuation compensation. The methods which take into account the statistics of the measured data are known as least squares methods and the method of implementation can be found in the Donner Users Manual (a supply of which is at this workshop).

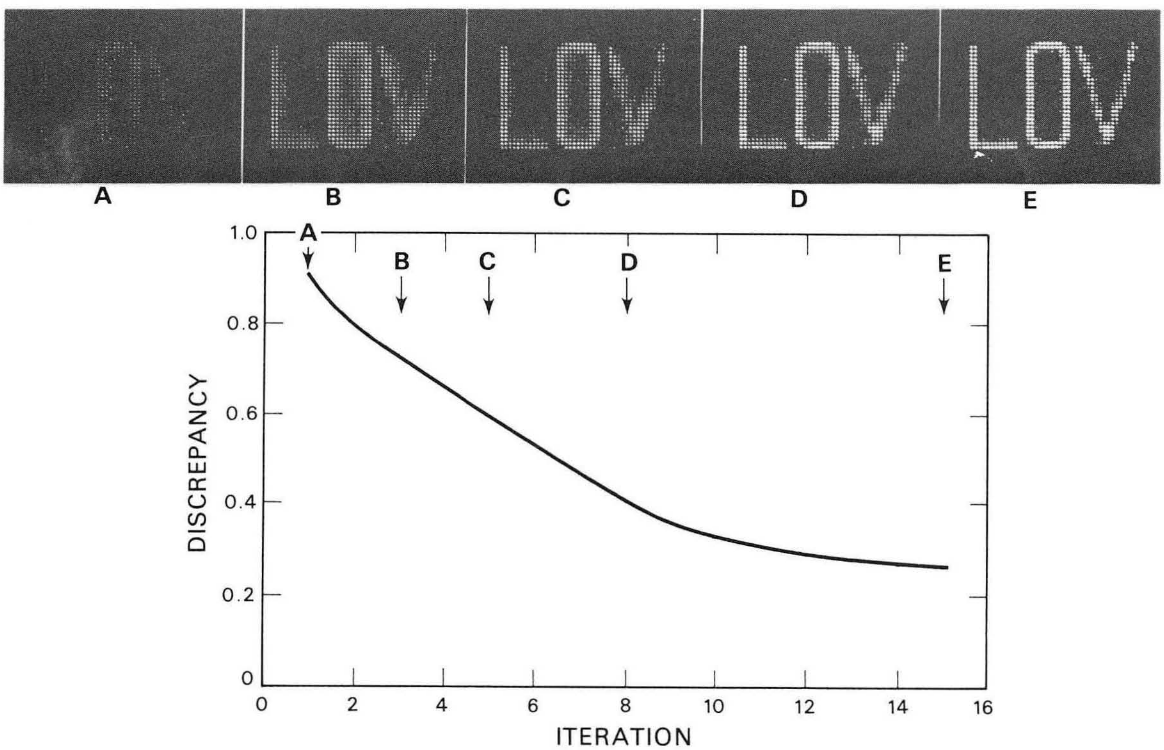

A_1	A_2	$\Sigma = 3$
A_3	A_4	$\Sigma = 7$
$\Sigma = 4$	$\Sigma = 6$	

If we estimated each element had the mean value of 10/4, we would note that $A_1' + A_2' = 5$, which is 5/3 greater than the measured value, thus we make a second estimate at the value for A_1 and A_2 of 3/5 (10/4) = 6/4; this gives an array with the first row modified as

		$\Sigma =$
		$\Sigma =$
$\Sigma =$	$\Sigma =$	

Clearly the values of A_3 and A_4 need to be increased, because their sum deviates from the measured value by 5/7. After adjusting these values by 7/5 (10/4) = 14/4, we have

		$\Sigma =$
		$\Sigma =$
$\Sigma =$	$\Sigma =$	

The sums of the vertical rows need adjustment to coincide with the measured values; thus after the first iteration, we have

		$\Sigma =$
		$\Sigma =$
$\Sigma =$	$\Sigma =$	

which gives one solution.

4. FOURIER PROJECTION THEOREM METHOD:

This method is used frequently in crystallography. In the medical community it is often confused with the Fourier filter or convolution method because of its intimate mathematical relationship to that method. The basis of the method is the Fourier projection theorem which states that the results of the Fourier transformation of a projection is the same as the values of the Fourier coefficients along a line through the two dimensional Fourier transform of an object. The line of values in 2-D Fourier space is oriented along the direction that the projection was taken. Thus (as illustrated below), if we take many projections, Fourier transform each, place the results in a 2-D array, and then do an inverse Fourier transform, we will have achieved a transverse section reconstruction.

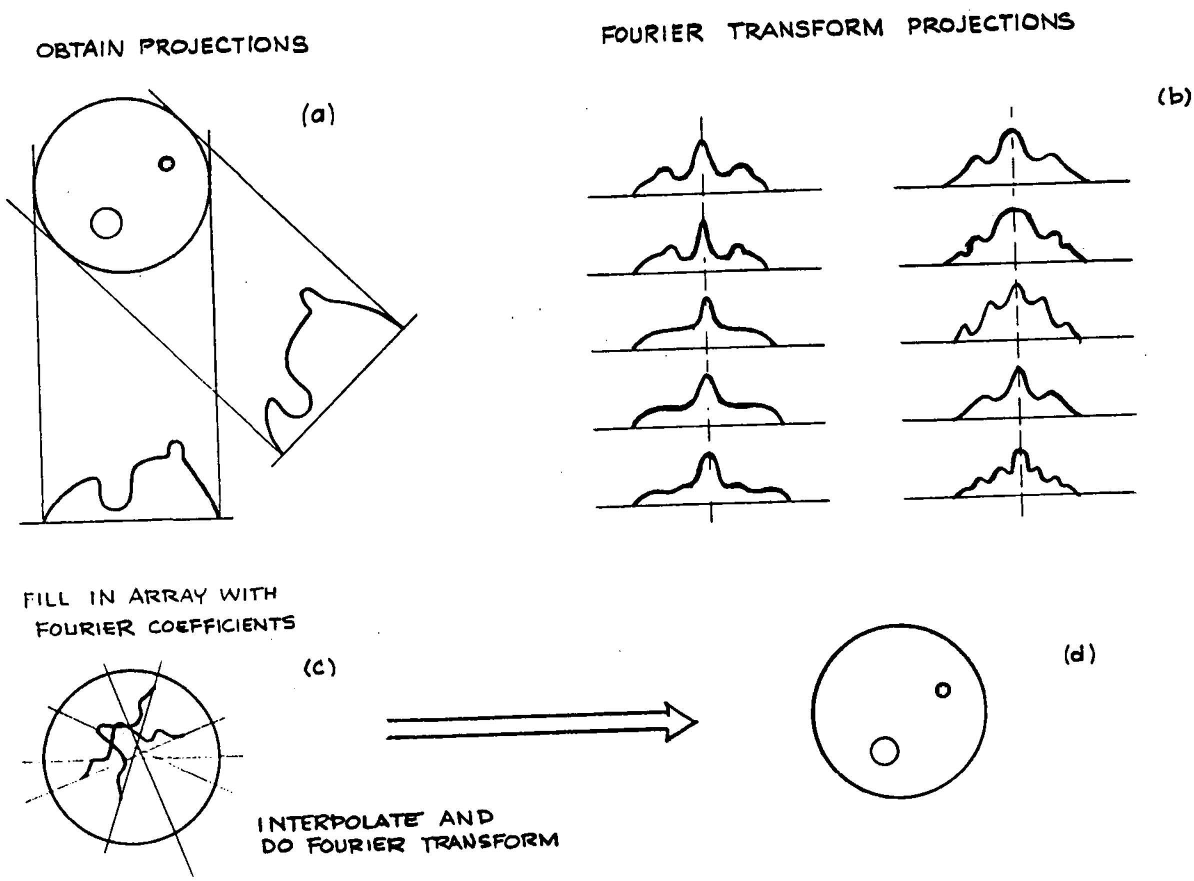

5. DIRECT MATRIX OR GENERALIZED INVERSE TECHNIQUES:

This method involves inverting a large matrix and matrix multiplication of the result with the projection values. The technique works only for perfect data and a sufficient number of independent measurements. For example if we set up the problem of exercise III as a group of equations for projections at 0° and 45°, we find it is possible to solve for the correct values using direct matrix techniques.

Consider the system of equations for views at 0° and 45°

$$\begin{array}{llllll} A_1 & & +A_3 & & =P_1 \\ & A_2 & & +A_4 & =P_2 \\ A_1 & & & & =P_3 \\ & A_2 & +A_3 & & =P_4 \end{array}$$

This system can be symbolized as

$$FA \quad =P \text{ with a solution given by}$$

For this case $$A \quad =F^{-1}\,P$$

$$F^{-1}= \begin{bmatrix} 0 & 0 & 1 & 0 \\ -1 & 0 & 1 & 1 \\ 1 & 0 & -1 & 0 \\ 1 & 1 & -1 & -1 \end{bmatrix}$$

The extension of this problem to real data and large arrays involves serious complications; for example, suppose there are sufficient data that the values in a section of say N x N picture elements can be determined by a linear system of simultaneous equations. At first glance, it would seem for a 64 x 64 array that 4096 simultaneous equations must be solved. Most investigations stop at this revelation and proceed to other methods discussed above. It is important to investigate this problem in more detail in the future before giving in to the notion that such a large matrix inversion is intractable. The direct-matrix method involves a matrix size equal to approximately

(N X N) • (no. of projections) • (no. of elements per projection).

The iterative methods can be considered as short-cuts to implementing this inversion, one step at a time, until a nearly exact answer is obtained. These methods have a role in problems of limited number of views, incomplete data and problems where *a priori* knowledge is available.

6. OPTICAL METHODS:

Reconstructionscan be performed using optical methods of filtering back projection data, or optical methods of performing Fourier transformations. The key to the methods is the fact that a lens performs a Fourier transformation of an object. The intensity distribution in the back focal plane is related to the modulus of the Fourier coefficients. This is the diffraction pattern of the object. Shown below is a way of implementing the FOURIER PROJECTION THEOREM using lenses.

MAGIC OF THE FOURIER PROJECTION THEOREM

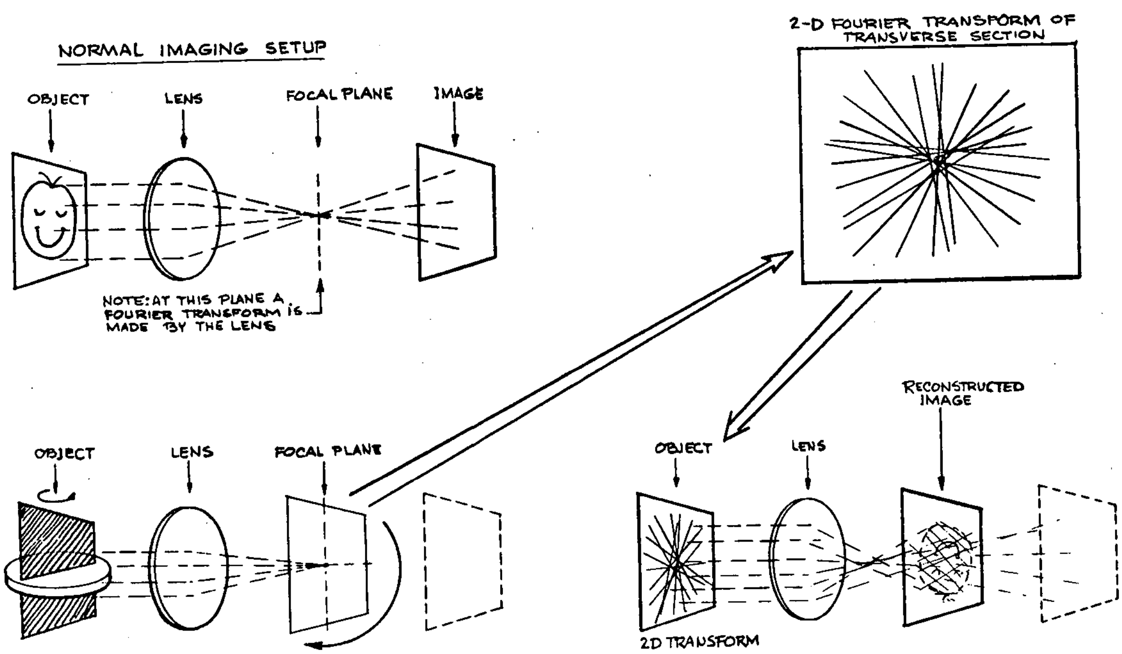

THE SINOGRAM

Another way of examining the projection and back projection problem is shown below. Optical subtraction methods on the sinogram before reconstruction have been used with some success to perform the de-blurring.

PROJECTION DATA TAKING

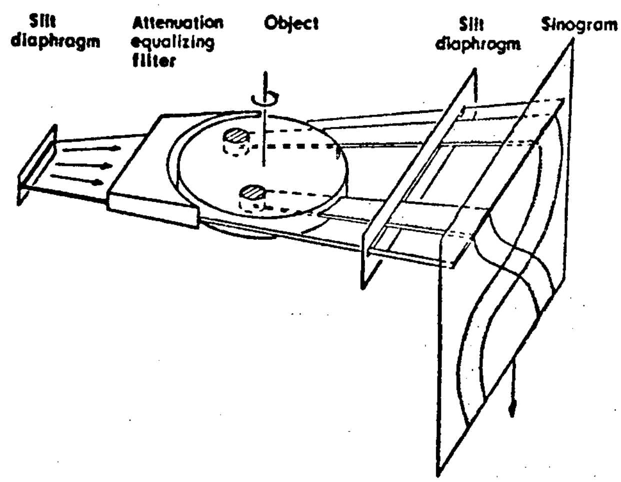

RECONSTRUCTION

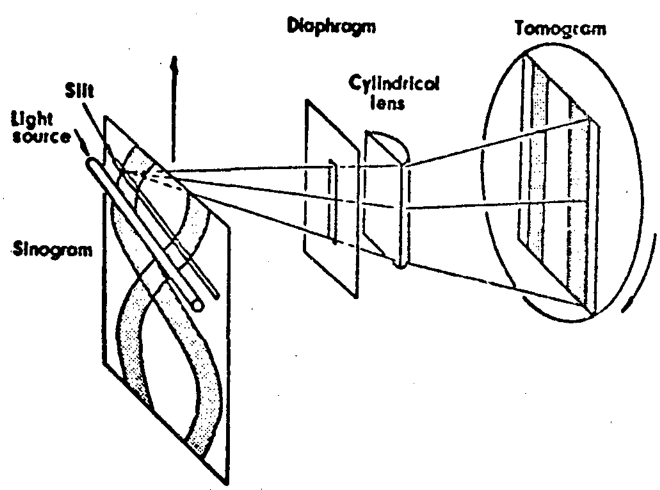

NUMBER OF VIEWS AND NUMBER OF SAMPLES

Using the methods discussed above, good results will be obtained if the density of sampling is adequate. The number of views needed for emission transverse sections is determined by the number of resolution elements across the image. By this rule of thumb an image with 64 x 64 resolution elements requires at least 64 views or projections at about 5° increments. A more exact estimate for the number of views needed is $\pi/2 \times D/a$ where D is the object diameter and a is the resolution.

For a good reconstruction the sampling interval of projections should be 2 times less than the desired resolution. This requirement is based on the sampling theorem.

Butterworth (F_{max} =32; node=12)

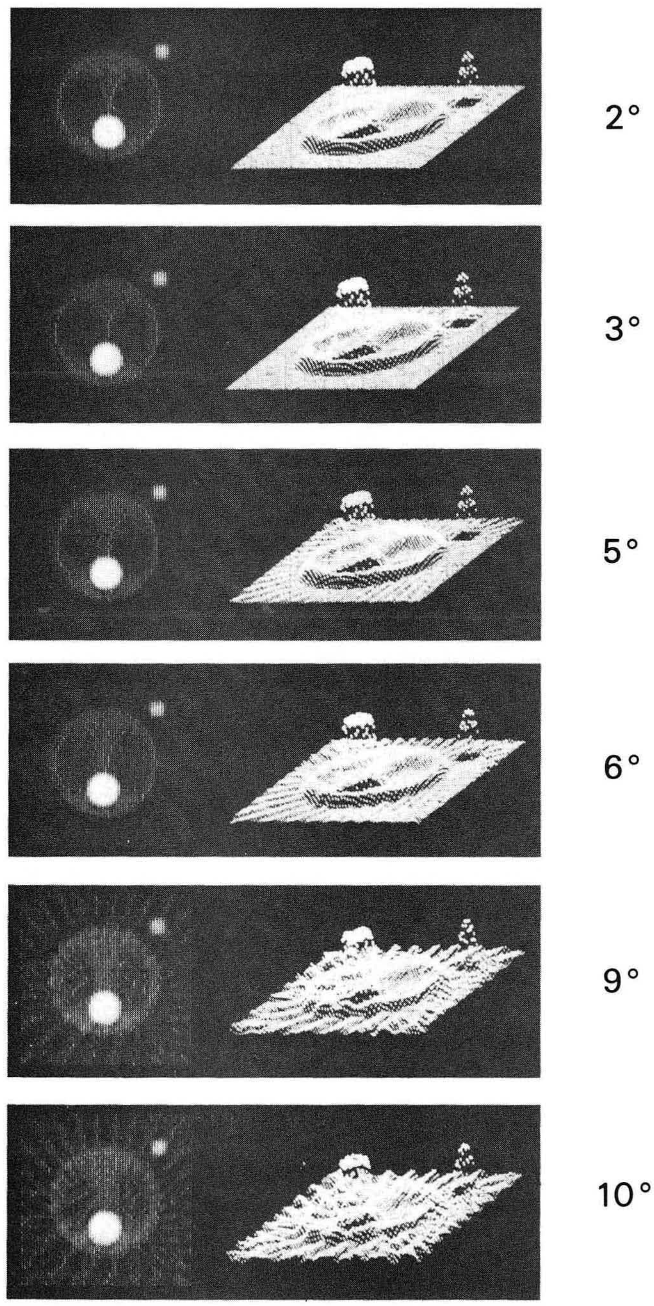

LOW STATISTICS OF ECT

Probably the most significant problem of ECT is the fact that we are severely limited in the number of events which can be detected with reasonable doses and practical imaging times. A TCT image represents about one billion detected photons (10^9), whereas the usual ECT image is one million events (10^6). Thus the ECT image represents 1000 times less data than the TCT image. The reasons for this difference lie in the fact that the patient radiation dose cannot be too great and the mode of detection in ECT requires single event analysis rather than photon current analysis used in TCT.

In this section, the relationships are presented between the number of detected events and the probable error or percent uncertainty in the quantitative values of ECT. The fractional uncertainty is also known as the noise to signal whose reciprocal is the signal to noise.

$$\frac{\text{Signal}}{\text{Noise}} = \frac{100}{\text{Percent Uncertainty}}$$

We cannot merely estimate the SNR in an ECT image from the number of events per resolution element using the usual formula of

$$\frac{N}{\sqrt{N}} = \sqrt{N}$$

because the process of reconstruction increases the uncertainty by a factor which is approximately equal to the square root of the number of resolution elements across the reconstructed image.

Total events – 1,200,000
Total resolution elements – 3000
400 events/element

Naive Prediction | Actual

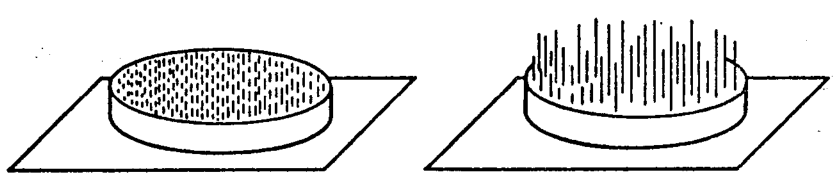

rms % uncertainty 5% | rms % uncertainty 44%

$$\boxed{\text{rms \%} = \frac{120\,(\text{no. resolution cells})^{3/4}}{(\text{total no. events})^{1/2}}}$$

If the resolution cell size is decreased (improved) by a factor of 2, then $2^3 = 8$ times more data are required to give confidence in the data similar to that before resolution improvement.

The formula for a uniform disc of activity is

$$\% \text{ rms uncertainty} = \frac{120 \cdot (\text{no. resolution cells})^{\frac{3}{4}}}{(\text{total no. events})^{\frac{1}{2}}}$$

and the formula for a target of increased uptake in the section of uniform activity is

$$\% \text{ rms uncertainty} = \frac{120 \cdot (\text{total no. events})^{\frac{1}{4}}}{\left(\begin{array}{l}\text{average no. events per} \\ \text{resolution cell in the} \\ \text{target}\end{array}\right)^{\frac{3}{4}}}$$

The diagram Pg. 29 gives the relationships between needed events and the effective number of resolution cells. Note that the effective number of resolution cells might be much smaller than the number of picture elements (pixels) because the number of pixels can be made large at the convenience of the computer or display system. For example, an image can be digitized at 64 x 64 or 128 x 128 or some other raster size. If the resolution is such that there are 64 resolution cells across the image then a calculation of the standard deviation using data from a 128 x 128 array will give erroneously optimistic results. The effective number of resolution elements for one organ in a uniform background is

$$\begin{array}{l}\text{effective number of} \\ \text{resolution cells}\end{array} = M_t + \frac{M_b}{C}$$

where M_t and M_b are the numbers of resolution cells which comprise the target and the background respectively; and C is the target-to-background contrast ratio.

Using the equation above for the effective number of resolution cells and the basic equation for the % rms uncertainty we can calculate the number of required events from

$$\text{Total no. events} = \left(\frac{120}{\% \text{ uncertainty}}\right)^2 (\text{effective no. resolution cells})^{\frac{3}{2}}$$

The result from this calculation will be the same as described in the graph below.

For most ECT images the effective number of resolution elements is 300 to 1000 thus the data needed for a transverse section with a SNR of 10 (% uncertainty of 10) ranges from 750,000 to 4,500,000.

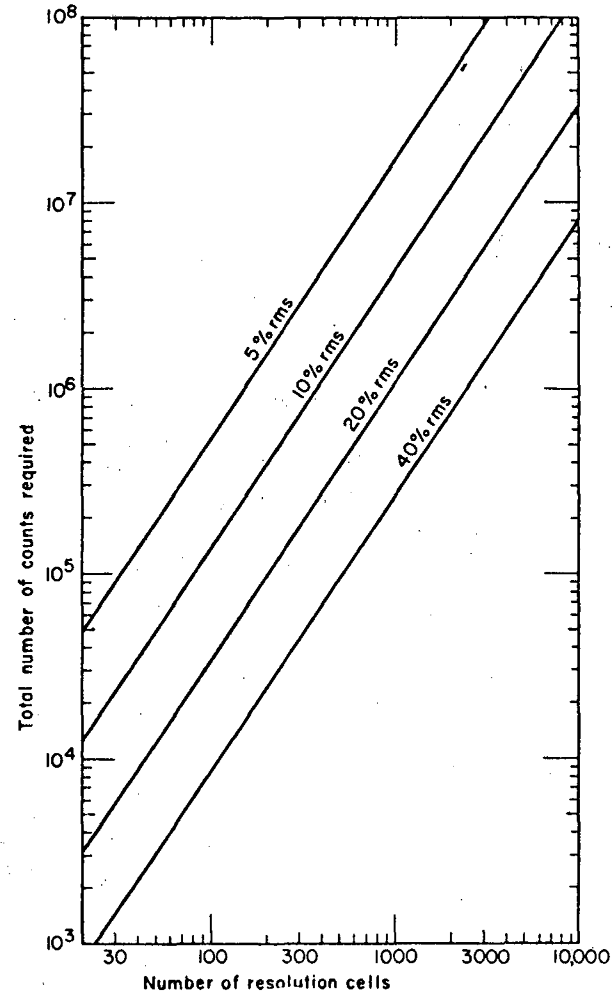

EXERCISE IV

What is the confidence you should have in the quantitative values of an ECT image with 100,000 events and 300 resolution cells?

THE ATTENUATION PROBLEM

This primer has been a general discussion of the methods of computing an image of an object from projections of information from that object. This is a straightforward problem for x-ray transmission computed tomography (TCT) but not quite so simple for emission computed tomography (ECT). The basic difference is that in TCT we compute the distribution of x-ray attenuation coefficients or x-ray density under conditions of a known transmission source position and intensity, whereas in ECT we must compute the source size and the source position as well as the attenuation between the source and the edge of the body. Thus we have a much more complicated problem in nuclear medicine. These differences are illustrated below.

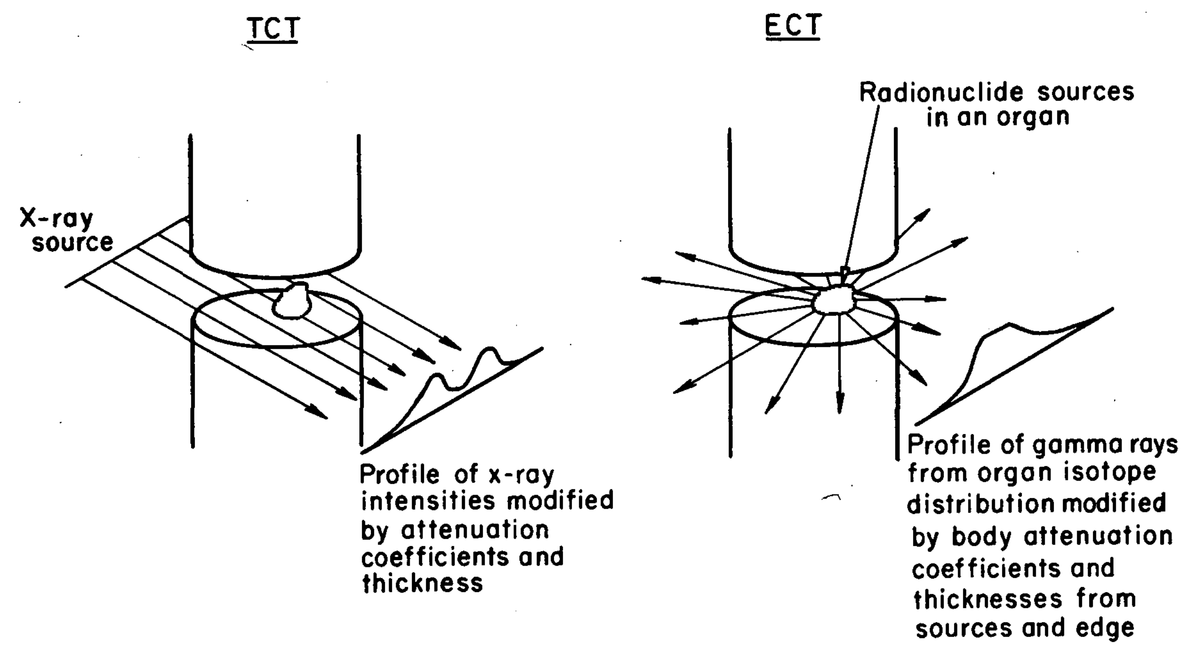

If we can find a way to compensate for the attenuation, then the algorithms discussed above will be effective in ECT. The effect of attenuation can be seen from the diagram below which illustrates what happens to a projection profile under conditions of ^{99m}Tc imaging.

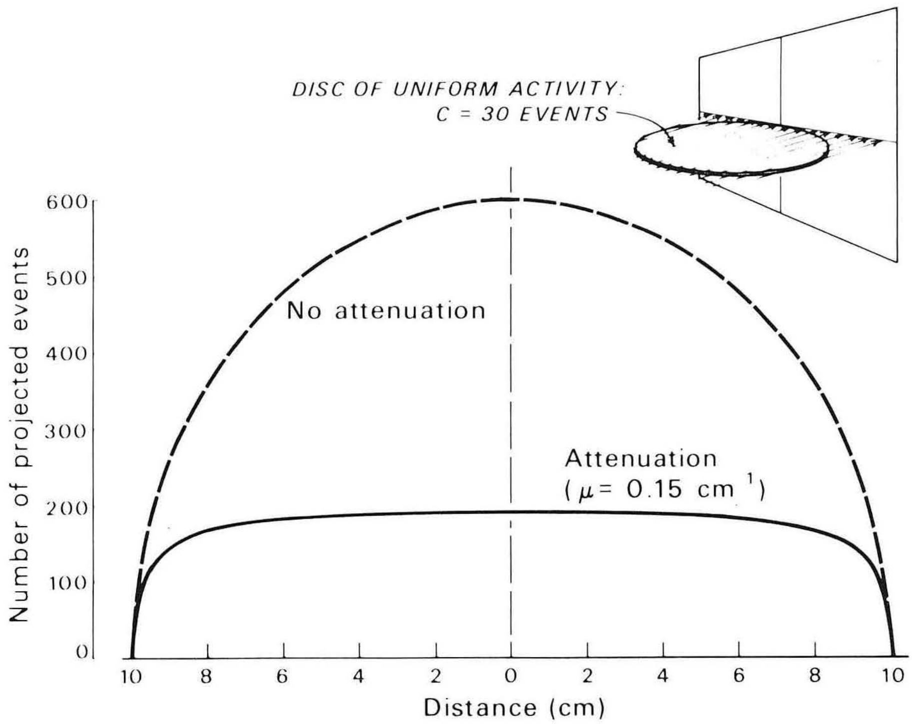

If we use the attenuated profile for reconstruction without any other modification the result will be a disc-like or concave distribution as shown below.

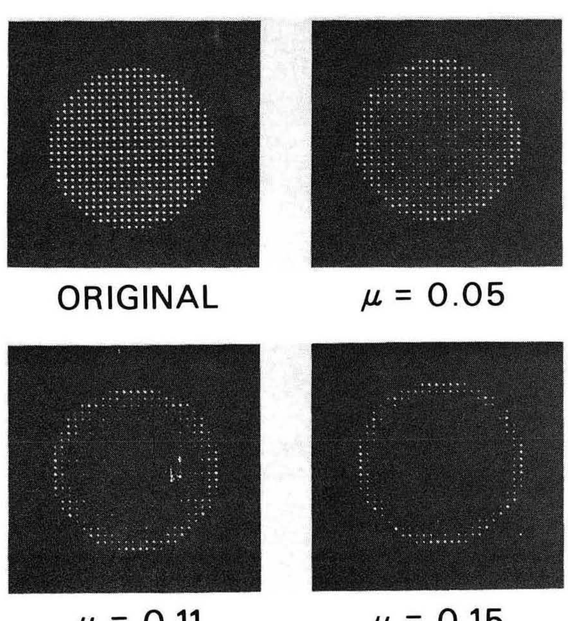

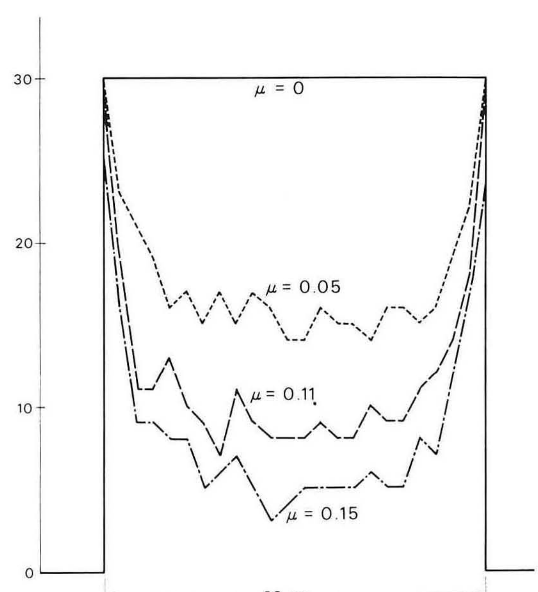

ATTENUATION COMPENSATION ALGORITHMS

As discussed on the previous pages, the attenuation of photons from a source in the body results in distorted projection data. For quantitative results, some method for compensating for this distortion must be used. The method for attenuation correction used in positron emission tomography is very simple because the effective attenuation of an object can be determined by performing a transmission scan before the emission scan. For single photons, the attenuation correction methods are more difficult.

Positron ECT Attenuation Correction

The act of detecting annihilation photons in coincidence leads to a multiplicative probability where for a source of unit activity anywhere in the body:

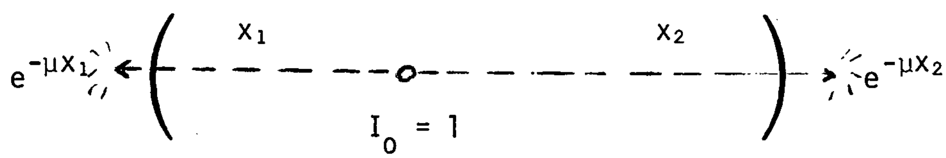

Coincidence detection means:

$$e^{-\mu x_1} \times e^{-\mu x_2} = e^{-\mu(x_1+x_2)} = e^{-\mu(\text{thickness})}$$

If we use a transmission source outside the body, the thickness can be determined. Thus by taking the ratio of the emission data over a particular ray to the attenuation for a transmission source, the proper compensation is obtained.

Because the transmission data have limited statistics the act of dividing transmission (TCT) information into emission (ECT) information of low statistics will result in even poorer reliability of the data than predicted by the statistics section above.

Single Photon ECT Attenuation Correction

Five methods of effecting attenuation compensation are given in this section. The first 4 do well under conditions of constant attenuation coefficient such as head and abdomen imaging. For variable attenuation coefficient distributions as found in the thorax, an iterative method is preferred.

METHOD I

Simple Array Modification

If the object being imaged has a uniform attenuation coefficient and is of known dimensions, then it is possible to correct the ECT image by multiplying each pixel by a known calibration factor determined from model studies or simulations. This is the method Kuhl and co-workers use with their single photon systems. The shape of the head or abdomen must be known very well for this technique to give good results on a variety of transverse sections.

METHOD II

Modification of Bin Values Before Convolution

This procedure involves multiplying the bin values for each projection by a factor $e^{+\mu d_k}$ where μ is the attenuation coefficient and d_k is defined in the diagram below. Imagine a line through the axis of rotation and parallel to the projection array. The value of d_k is the distance between that line and the edge of the object.

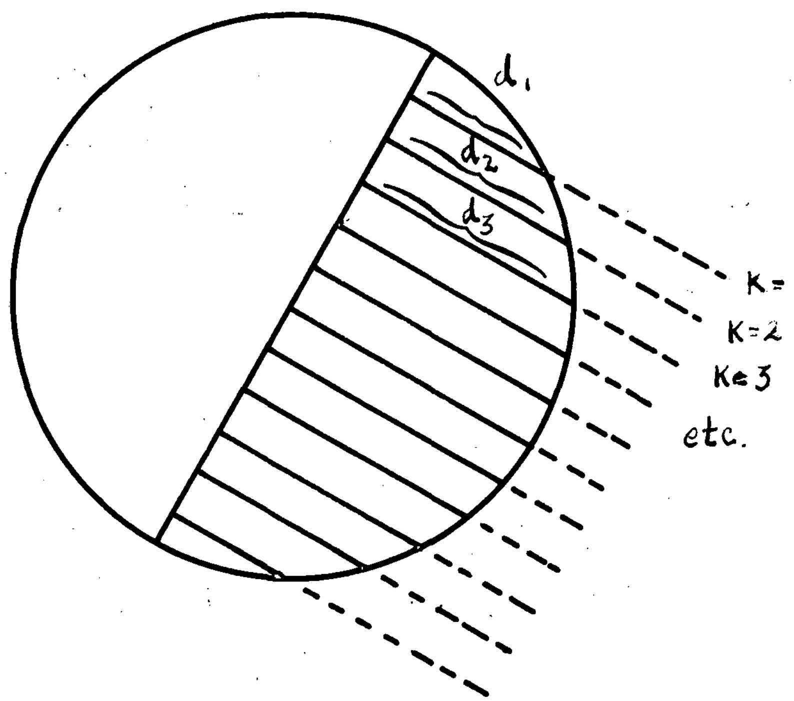

After modifying each value for every bin of each projection angle, a conventional convolution reconstruction is used with a kernel similar to the Shepp-Logan, Chesler, or RAM-LAK kernel. This method also suggested by Tretiak works well for positron photons of μ = 0.096 or ^{99m}Tc photons of μ = 0.150. (Actually 2x the number of pixels are used to effect μ = 0.075) according to Gullberg (Ph.D. thesis, 1978).

METHOD III

Modification of the Geometric Mean

A third method applicable to situations of constant attenuation coefficient correction involves first forming the geometric mean of projection bin data by multiplying opposing projection rays by one another, then taking the square root. To this modified projection a hyperbolic sine correction is applied, then the convolution reconstruction method is used. The "sinh" correction factor is:

$$\frac{e^{x}\ fx}{\sinh\ (x)}$$

where x = attenuation coefficient x thickness/2 and f is set from 0.5 to 0.75 depending on the relative amount of activity along the projection line being modified. We have had good success with this technique. The method of finding the thickness of the object for each projection line involves estimation of the edges of the object from an initial reconstruction before applying the "sinh" correction.

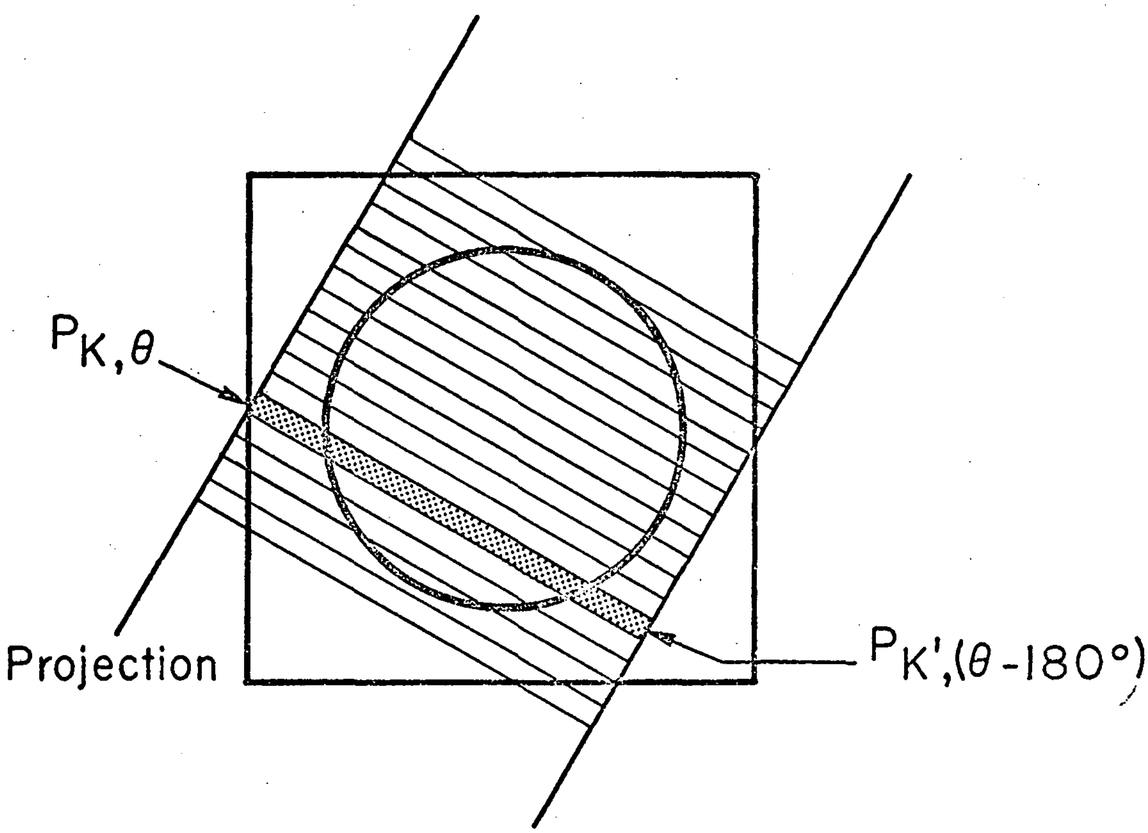

$$\text{MODIFIED PROJECTION} = \sqrt{P_{K,\theta} \cdot P_{K',\theta-180°}}\ (\text{"sinh" correction})$$

METHOD IV
Iterative Modification of Pixels

For a straightforward ECT reconstruction, we know the value of each pixel is low because the projected values were modified by an attenuation in accord with the distance between the pixel and the object edge along each ray which passes through that pixel. This modulation is given by

$$e^{-\mu d_\ell}$$

where d_ℓ is the distance along a particular ray denoted by ℓ. The overall average modification of the source in a particular pixel is merely the sum of these separate modifications divided by the number of projections m. Thus,

$$\frac{\sum_{\ell} e^{-\mu d_\ell}}{m}$$

The method of correction suggested by Chang (1978) involves first performing a reconstruction. Each pixel value $A_{i,j}$ is modified by

$$A_{i,j}^{new} = A_{i,j}^{old} \left(\frac{1}{\frac{1}{m} \sum_{\ell} e^{-\mu d_\ell}} \right)$$

Then the modified data are reprojected and the differences between the reprojected bin values and the measured projections are determined. These "difference projections" are used to reconstruct an error image which, when added to the modified image, gives a good result for constant μ.

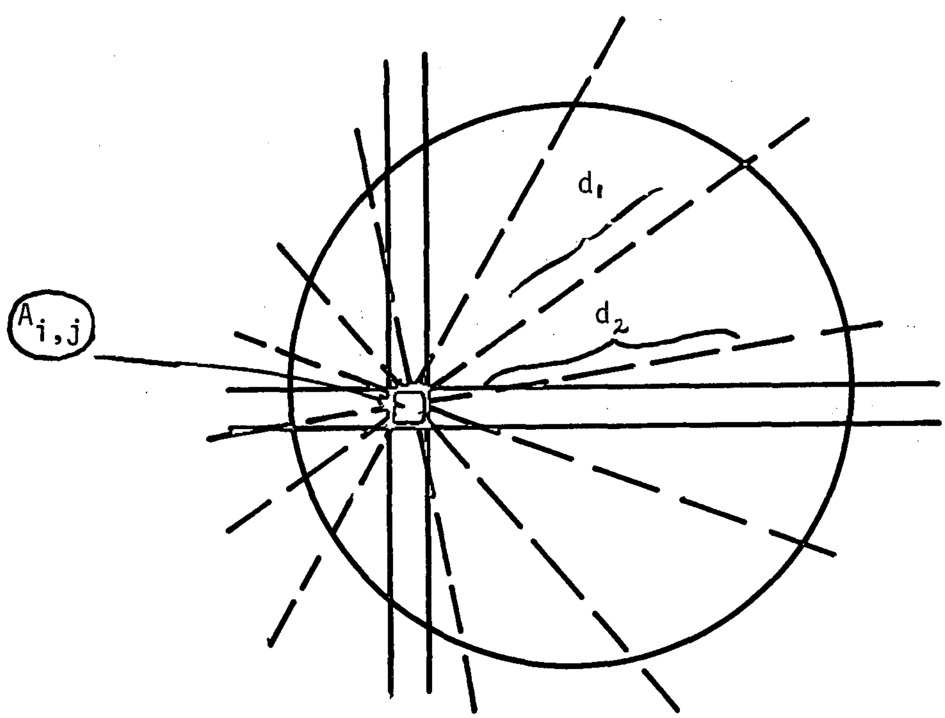

METHOD V.

Iterative Least Squares Weighting Factors

The iterative least squares method is somewhat similar to the iterative method given in the example on Page 19 except weighting is incorporated by taking into account the standard deviation of the data and, in the case of single photon ECT, by incorporating attenuation coefficient weighting factors into the reconstruction. The method is shown below as a flow diagram.

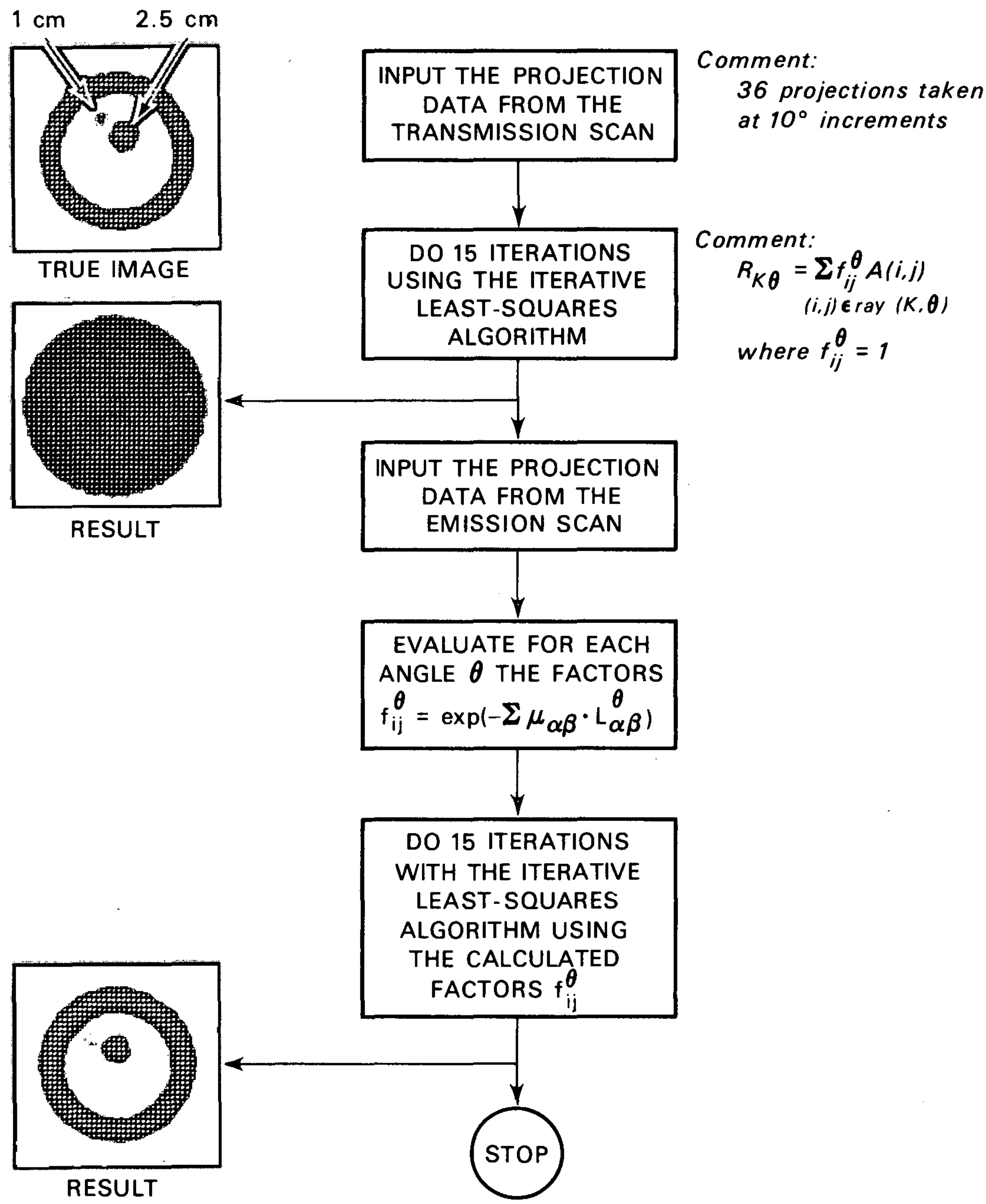

THE SCATTER PROBLEM

For single photon ECT as well as positron ECT, unwanted scattered radiation events enter the collected data. Single photon systems attempt to discard scattered data by pulse height selection and collimation. For positron annihilation photons, scatter is minimized basically by judicious shielding and to only a limited extent by a low threshold pulse height selection. In both types of imaging we can expect 10% or more of the collected data will be unwanted data resulting from some scattering in the attenuating medium. For positrons, these scatter coincidences are often confused with accidental coincidences which also have about 10% or more contributions to the total number of events. The accidental coincidences can be removed by electronic tricks; however, the scattered coincidences are more difficult to remove from the ECT image.

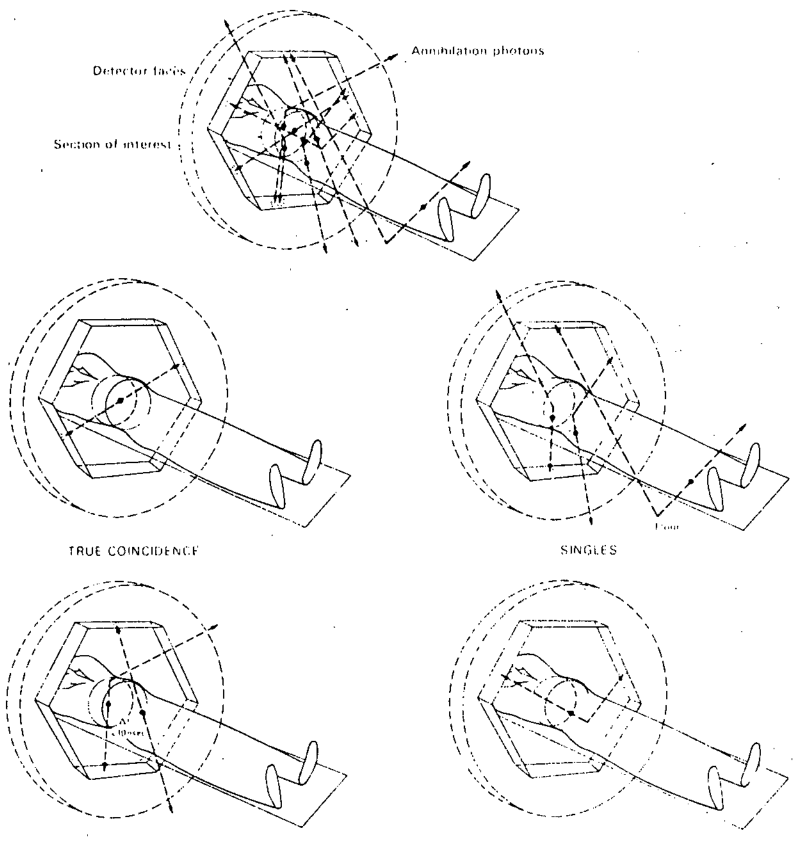

For a true coincidence rate of 5000 sec^{-1} (about 1 mCi/1-cm thick section), we expect 500 events sec^{-1} as accidental coincidences, 500 sec^{-1} as scattered coincidences and 1 million sec as single photon interactions. This is the usual situation for PETT type devices, ring detectors, and parallel plane positron-imaging devices, such as the MGH positron camera, Searle Radiographics positron camera, or wire chambers. The basic difference in these devices is the saturation limit.

This work was supported by the U.S. Department of Energy under Contract No. W-7405-ENG-48.

SOME BASIC REFERENCES

ALGORITHMS

Budinger, T.F. and G.T. Gullberg. Three-dimensional reconstruction in nuclear medicine emission imaging. IEEE Trans. Nucl. Sci. NS-21:2-20, 1974.

Gordon, R. and G.T. Herman. Three dimensional reconstruction from projections: A review of algorithms. Int. Rev. Cytol. 38:111-151, 1974.

Huesman, R.H., et al. Users Manual - Donner Algorithms for Reconstruction Tomography. Lawrence Berkeley Laboratory Publication PUB-214, 1977.

Budinger, T.F., G.T. Gullberg and R.H. Huesman. Emission computed tomography. In Image Reconstruction from Projections: Implementation and Applications, ed. by G. Herman. Springer-Verlag, New York (in press).

SINGLE PHOTON vs POSITRON

Budinger, T.F., et al. Emission computer assisted tomography with single-photon and positron annihilation photon emitters. J. Computer Assisted Tomography 1:131-145, 1977.

Phelps, M.E. Emission computed tomography. Seminars Nucl. Med. 7: 337-365, 1977.

POSITRON

Phelps, M.E., et al. ECAT: A new computerized tomographic imaging system for positron-emitting radiopharmaceuticals. J. Nucl. Med. 19: 635-647, 1978.

Brownell, G.L., J.A. Correia and R.G. Zamenhof. Positron Instrumentation. In Recent Advances in Nuclear Medicine, ed. by J.H. Lawrence and T.F. Budinger. Grune & Stratton, New York, 1977, pp. 1-49.

Ter-Pogossian, M.M. Basic principles of computed axial tomography. Seminars Nucl. Med. 7:109-128, 1977.

STATISTICS

Budinger, T.F., et al. Quantitative potentials of dynamic emission computed tomography. J. Nucl. Med. 19:309-315, 1978.

ATTENUATION

Budinger, T.F. and G.T. Gullberg. Transverse Section reconstruction of gamma-ray emitting radionuclides in patients. In Reconstruction Tomography in Diagnositc Radiology and Nuclear Medicine, ed. by M.M. Ter-Pogossian, et al. University Park Press, Baltimore, 1977, pp. 315-342.

Walters, T.E., et al. Radionuclide axial tomography with correction for internal absorption. In Information Processing in Scintigraphy, ed. by C. Raynaud and A. Todd-Pokropek. Comissariat à l'energie atomique, Orsay, France, 1976, pp. 333-342.

Chang, L.T. A method for attenuation correction in radionuclide computed tomography. IEEE Trans. Nucl. Sci. NS-25:638-643, 1978.

TECHNICAL INFORMATION DEPARTMENT
LAWRENCE BERKELEY LABORATORY
UNIVERSITY OF CALIFORNIA
BERKELEY, CALIFORNIA 94720